Model development and testing of magnetic flux within a small-scale Hall-effect thruster

Henry, Z., Sitler, R., Russo, D., Decat, A., Weinstock, N., Sommer, D., Verdes, A., Morrow, C., Teale, C., Nelson, N., Boudreau, F.

I. Background

Since the 1960s, there has been a rising interest in various types of electric propulsion (EP) systems. Their increasing popularity has largely been due to their incredibly high efficiency and specific impulse,[1,2] allowing them to carry larger payloads to more distant regions of space than their chemical rocket counterparts. EP systems function by accelerating ionized gas away from the spacecraft and thus, by Newton's third law, generating thrust. While there are many types of EP systems, there are two main ones in use today: the ion thruster and the Hall-effect thruster.[2] The ion thruster generates ions in a chamber by various means and accelerates them through a potential field across a grid before discharging and neutralizing them. The Hall-effect thruster (Hall thruster, HET), on the other hand, both generates plasma and accelerates it by a cross-field inside the discharge chamber.

The large appeal to HETs are their comparative simplicity and relatively high thrust precision, being capable of producing from micronewtons to newtons of thrust. In the United States, this type of thruster has not been of major interest until fairly recently, with the first HET on a US mission occurring in 1998 on NROL-8, and the second in 2005 on NSS 10.

While their popularity is still low relative to conventional chemical propulsion systems, HETs show a lot of promise as being reliable and safe propulsion systems for future use, when it becomes possible to manufacture high thrust systems for a lower price. An issue which is encountered in small HET systems, however, is that it is difficult to completely ionize all of the propellant entering the discharge chamber. This causes a loss in thrust as well as efficiency, so it is necessary for optimization of the magnetic field within the discharge chamber. As a first step for this, we have developed a mathematical model of the electromagnets inside the thruster for comparison to experimental data which is to be collected in the future.

II. Design

Our design was based on a large number of thrusters which were encountered during our research. Several aspects which allowed for easy modification were incorporated in order to allow for a wider variety of experimentation. The isometric view of our design is pictured in Figure 1. The backplate is 7075 Aluminum, chosen for its high resistance to corrosion. The discharge chamber is composed of a number of Alumina rings for the purpose of easy variations in chamber length, and they are held in place by the pressure imparted on them by the inner and outer magnetic circuit rings. All components of the magnetic circuit are made from AISI 1010 steel, with a relative permeability on the order of 100-900, depending on the active field. Another benefit to this choice is that the field strength for saturation of the material is 100 times greater than our desired field strength. Our anode plate is made from 316 stainless steel, chosen for its low relative magnetic permeability which is quite close to that of air. The screws and nuts used to hold everything in place are also made from 316 stainless steel. The magnet cores sit on these screws and are wrapped with 28 AWG copper magnet wire with a turn density of about 54.6 turns per centimeter.
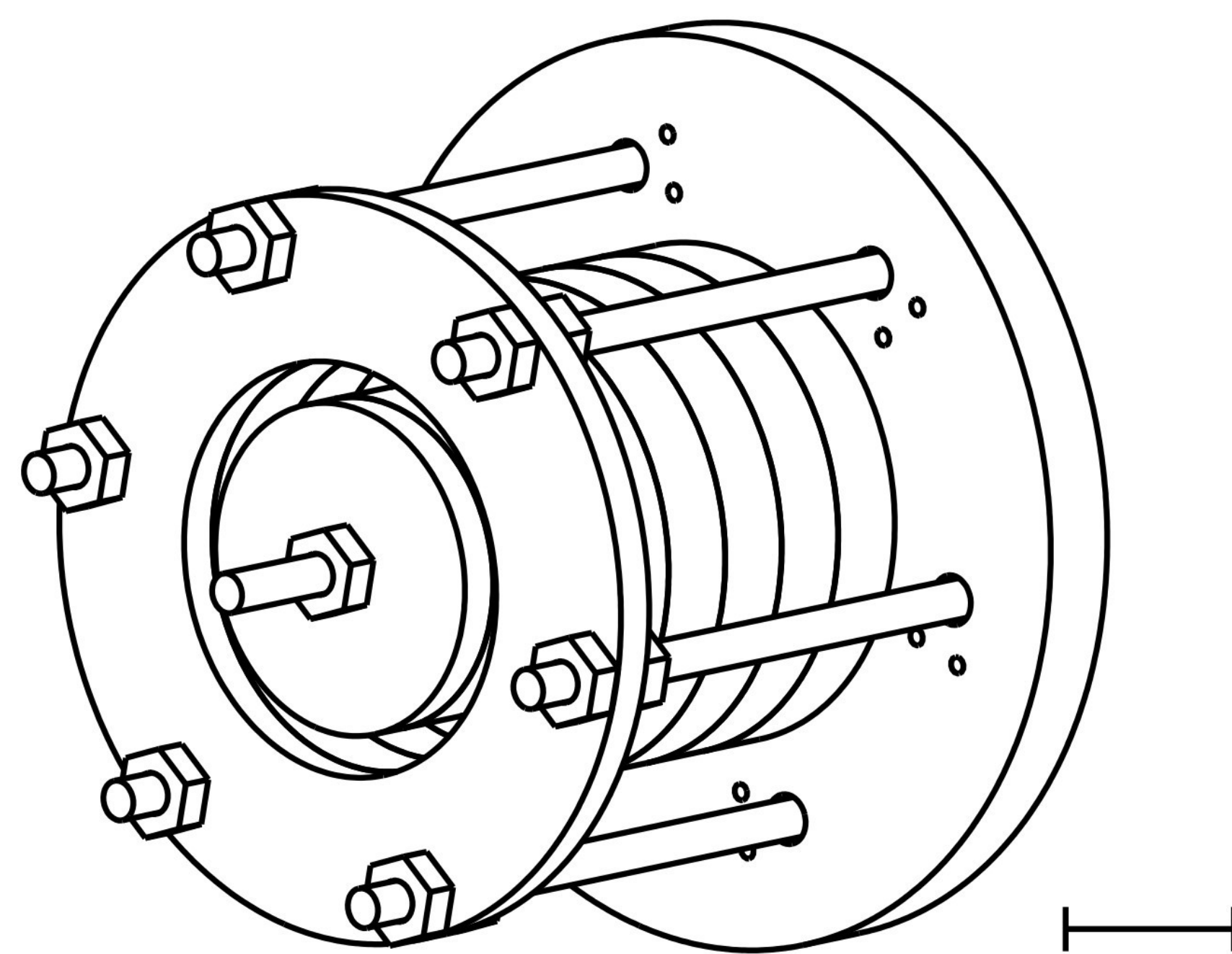

Figure 1: Isometric view of thruster design.

III. Mathematical Model

In order to model the magnetic field for the HET, we must develop a model for the magnetic potential of a solenoid, denoted (**A**). To start this process, we examine a solenoid of single loop with radius 1.2mm (as per design constraints) with a current of 1 ampere (design range of 1 mA to 1A). Once a model of the magnetic potential is produced for a single loop, then using:

$$\mathbf{B} = \nabla \times \mathbf{A}$$

a magnetic field, denoted (**B**), can be determined. By evaluating this expression over the height of a coil, a true representation of the magnetic field can be obtained. Finally, using the principle of super-position we can model the total magnetic field around the HET.

To accomplish this, two approaches were determined: analytically or numerically. Since our HET had finite geometry and the goal is to collect data, a numerical approach is used. This numerical approach stems from an expansion of:

$$A_\phi(r, \theta) = \frac{\mu_0}{4\pi} \frac{4Ia}{\sqrt{a^2 + r^2 + 2ar\sin\theta}} \left[\frac{(2 - k^2)K(k) - 2E(k)}{k^2}\right]$$

from Jackson's third edition of Classical Electrodynamics. The approximation, also from Jackson is as follows:

$$A_\phi(r, \theta) = \frac{\mu_0 Ia^2 r \sin\theta}{4(a^2 + r^2)^{3/2}} \left[1 + \frac{15a^2r^2 \sin^2\theta}{8(a^2 + r^2)^2} + \cdots\right]$$

Using this numerical approximation, Figures two was produced. Also from this expression, the approximate magnetic fields in the radial and angular directions were found.[4]

$$B_r = \frac{\mu_0 Ia^2 \cos\theta}{2(a^2 + r^2)^{3/2}} \left[1 + \frac{15a^2r^2 \sin^2\theta}{4(a^2 + r^2)^2} + \cdots\right]$$

$$B_\theta = -\frac{\mu_0 Ia^2 \sin\theta}{4(a^2 + r^2)^{5/2}} \left[2a^2 - r^2 + \frac{15a^2r^2 \sin^2\theta(4a^2 - 3r^2)}{8(a^2 + r^2)^2} + \cdots\right]$$

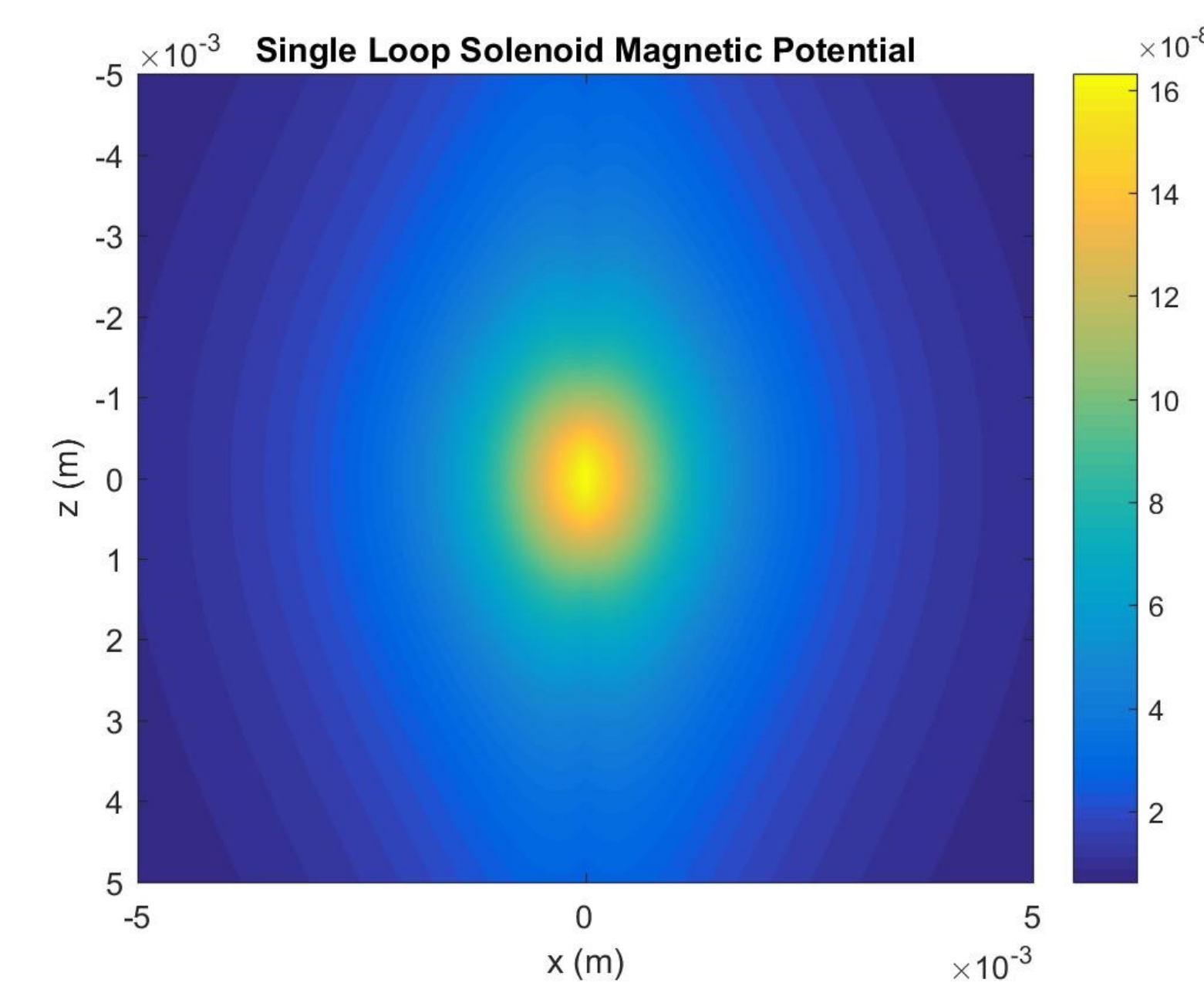These numerical approximations of the magnetic fields produced figures three and four, respectively.

Figure 2: This is an XZ intensity graph that shows how the magnetic potential varies around a single loop with current of 1 ampere and a loop radius of 1.2 mm
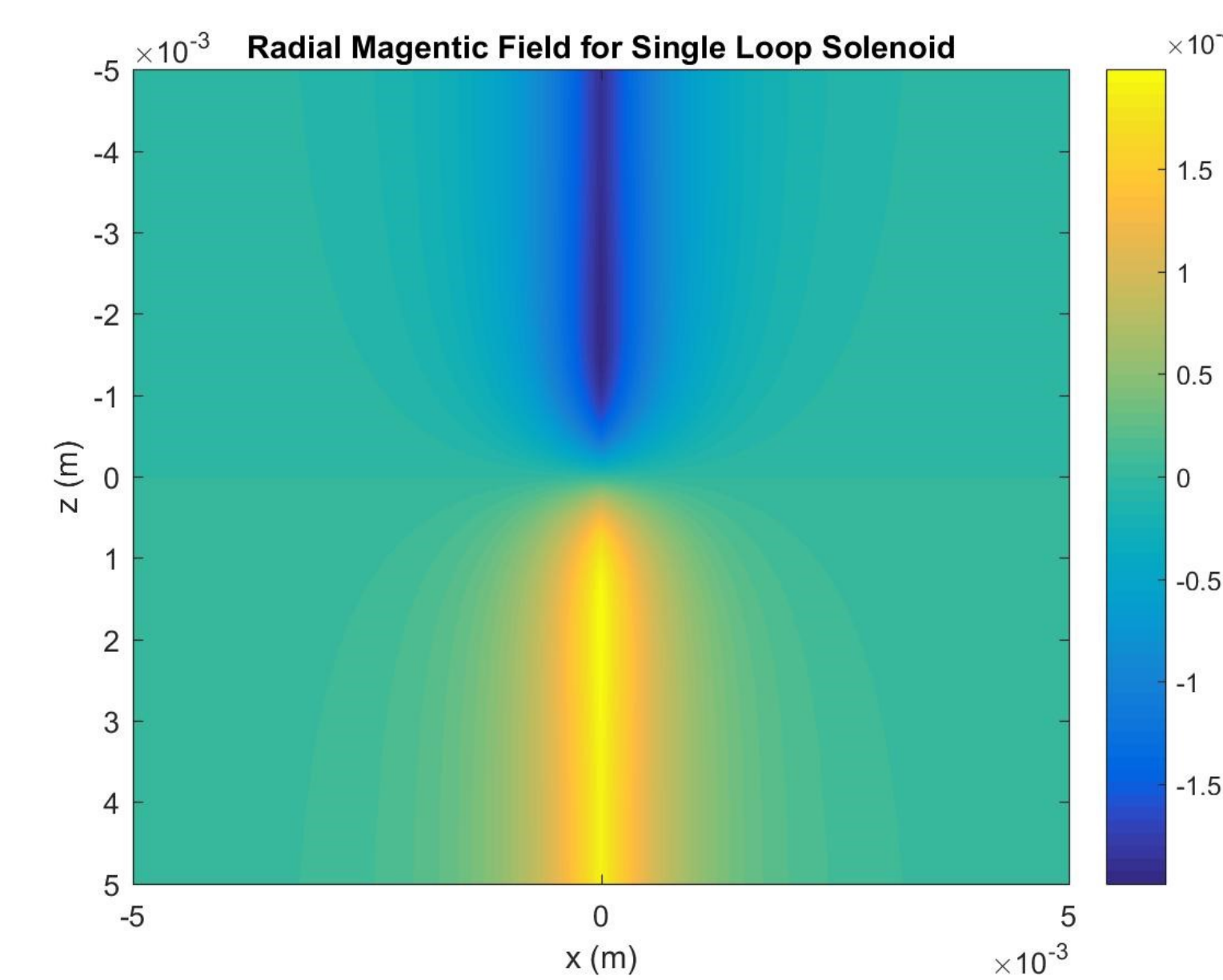

Figure 3: This is an XZ intensity graph of the radial magnetic field produced by a single loop with the same characteristics as in Figure 1. The values on the scale on the right are in Tesla.
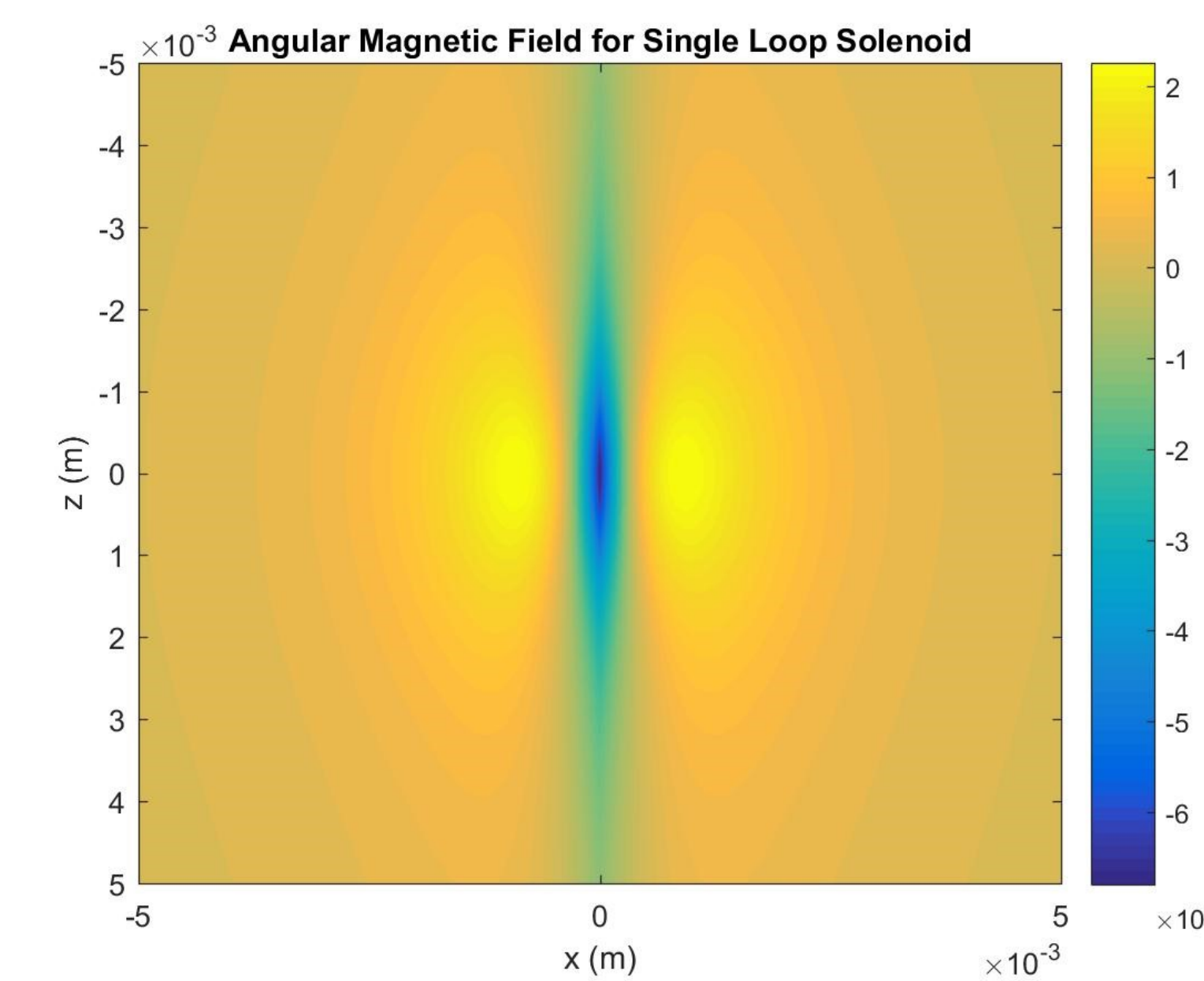

Figure 4: This is an XZ intensity graph of the angular magnetic field produced by a single loop with the same characteristics as in Figure 1. The values on the scale on the right are in Tesla.

IV. Data Acquisition

To measure the magnetic flux density inside the chamber, we will be using a hall probe. A hall probe is a small device which makes use of the hall effect, a physical phenomena which creates a voltage across a plate placed in a magnetic field. They are used to detect the normal B-field component to the flat side of the probe.
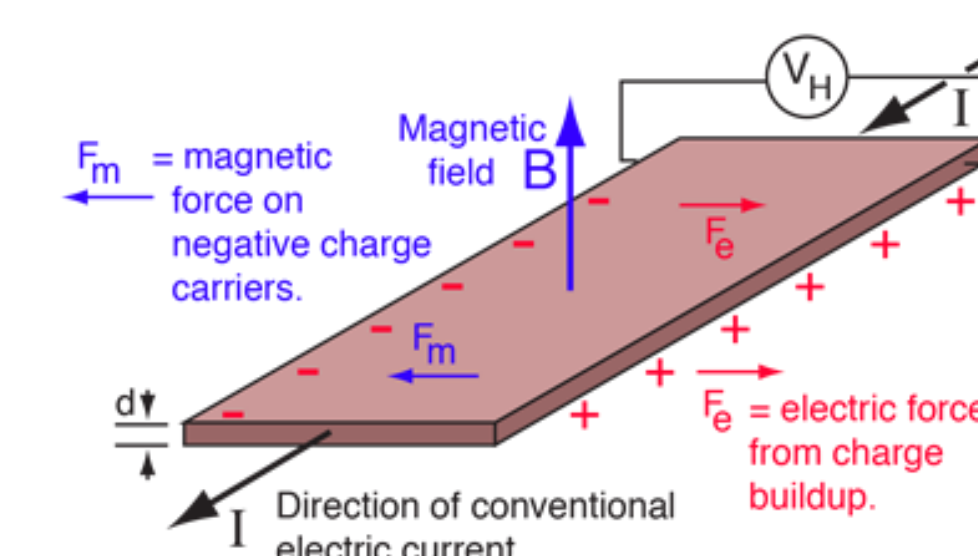

Figure 5: Hall effect diagram[3].

The operation of the probe is as follows. A positive voltage is applied to the probe. At this time, the electrons travel in a straight line, from this applied voltage to the neutral terminal. Once a magnetic field is applied to the probe, the path of the electrons is modified. This force acting on them is known as the Lorentz Force. As this happens, electrons are pushed to one side of the probe, creating an electric potential difference between the two sides. The size of this difference is directly related to the B-field, and is what is actually measured in the probe. A diagram of this process is depicted in Figure 5.

We have elected to use a RobotDyn hall probe for the experiment, due to its two main advantages in addition to its low cost. The first is the potentiometer on the circuit, which allows for calibration of the sensor. The other is the integrated circuit provided, which includes an LM358 operational amplifier as part of the circuit. When wiring a hall-probe, several components are used in conjunction to get a proper reading, and the integrated circuit has all of these included. This greatly simplifies assembly of the measurement system, only requiring four wires to be attached to its pins.

Four probes will be used to collect data in order to collect data with probes oriented at different angles. The four probes will be placed in a circular pattern on a PVC endcap, and the endcap will be attached to the central screw of the thruster in order to hold it steadily (see Figure 1). Using a variety of measurement angles allows us better understand the field geometry, and be able to detect then correct any discrepancies. Rotating around the thruster will allow for the ability to confirm that the field is uniform and the field across the thruster is around 0.020 [T].

The device the probes are connected to is an Arduino Mega. This device was picked due to its ease of use. It has plenty of analog and digital pins to use, allowing for the microcontroller to be used in the future for other parts of this project. The 5 [V] rail will be used to power the probes. The Arduino will be used to measure the potential difference of each probe, at a sample rate of 100 [Hz].

The following equation is used to determine the flux density[3]:

$$V_h = \frac{I}{qnd} B$$

Here, V_h is Hall voltage, the potential difference created by the B-Field, I is the current going through the probe, q is the electron charge, n is the mobile charge carried per unit volume, d is the thickness of the probe, and B is the magnetic flux density.

V. Future Developments

Due to manufacturing delays, the experiment was not performable in the time frame of our funding. Thusly, the first step in the future of this will be to construct the test thruster and take measurements of the magnetic field as previously described, then improve upon our mathematical model of the magnetic circuit. When this is completed, the developed modeling software will be used to optimize the physical geometry of the components in the circuit.

After this, the most important acquisition before a test fire will be a Hollow Cathode—a major component to many EP systems. With this, we will be able to put the design to a real test which will reveal whether undergraduates are truly capable of doing this level of work.

Another development will be the addition of a new sub-team within the ERPL Plasma division, tasked with educating newcomers to the team about basic plasma physics through both mathematics and laboratory demonstrations of plasmas. We have access to a number of experiments for use with LabView by courtesy of Dr. Charles Lee of the Physical Sciences Department. After several years of growth, it should be possible to begin a 6-to-10 year proper design and development project led by a self-motivated, self-educating, self-sustaining undergraduate team. Ideally, there should be an addition of courses on the topic to the ERAU curriculum, and potentially a new degree program which mixes the relevant aspects of aerospace engineering, electrical engineering, and engineering physics.

References

[1] Goebel, D.M., and Katz, I. *Fundamentals of Electric Propulsion: Ion and Hall Thrusters*. John Wiley & Sons, Inc: Hoboken, NJ, 2008; Chapter 2, p 23; Chapter 7, p 329-337.

[2] Jahn, R.G. *Physics of Electric Propulsion*. McGraw-Hill, Inc: New York, NY, 1968; Chaper 1, p 2-11.

[3] Hall Effect, HyperPhisics. Georgia State University. http://hyperphysics.phy-astr.gsu.edu/hbase/magnetic/Hall.html (accessed April 2018).

[4] Jackson, J.D. *Classical Electrodynamics*. Third Edition. John Wiley & Sons, Inc: Hoboken, NJ, 1998; Chapter 5, p 182-183.

EMBRY-RIDDLE
Aeronautical University

ERPL

ignite
CREATE · RESEARCH · CHANGE